

## COMBINED EFFECTS OF EMBEDDED ANGLE AND PILE SPACING ON LOAD RESPONSES OF MICROPILES IN SANDS

Doohyun Kyung<sup>1</sup>, Junhwan Lee<sup>2</sup>, Garam Kim<sup>3</sup>, Daesung Park<sup>4</sup>, Daehong Kim<sup>5</sup>

### **ABSTRACT**

The Micropile technology has evolved continuously since first introduced in the 1950s. The performance of group micropiles change with various factors including pile length, pile spacing, pile embedded angle, and pile installation method. While the performance of group micropiles have been investigated by many researchers, the combined effects of various parameters on the load response of group micropiles have not been fully clarified yet, requiring further investigation. In the present study, the effect of embedded angle and pile spacing of group micropiles on the load capacity and induced settlement were investigated experimentally. An experimental testing program was established to measure loads and settlements of various foundation types including mat, group micropiles and micropiled-raft under axial loading conditions. Test results are then presented with discussions on the combined effects of pile spacing and embedded angle of micropiles.

KEYWORDS: Micropile, axial load test, sand, mat, group micropile, micropiled-raft

### **INTRODUCTION**

Micropiles are generally defined as piles of small diameter less than 300 mm. The micropile technology has evolved continuously since first instructed in 1950s. The micropile foundations can be classified as Cases 1 and 2 depending on supporting mechanism and classified into Types 1 to 4 according to the grouting method (FHWA2005).

Micropiles are generally regarded as frictional piles ignoring the end bearing capacity primarily due to small-diameter cross-section. As micropiles are installed in group, the consideration of group efficiency is important, which is affected by various foundation configuration conditions.

The mechanical behavior of group micropiles differs and changes with various factors such as pile length, pile spacing, pile embedded angle, and pile installation method. Lizzi et al. (1979) investigated the group efficiency of axially loaded micropiles focusing on the effect of pile spacing. The positive group efficiency ratio, higher than 1, was observed for pile spacings from 2 to 7D where D is the diameter of micropiles.

---

<sup>1</sup> Doohyun Kyung, Ph.D. candidate, School of Civil and Env. Eng., Yonsei University, Seoul, Korea

<sup>2</sup> Junhwan Lee, Professor, School of Civil and Eng. Env., Yonsei University, Seoul, Korea

<sup>3</sup> Garam Kim, Graduate Research Assistant, School of Civil and Env. Eng., Yonsei University, Seoul, Korea

<sup>4</sup> Daesung Park, Graduate Research Assistant, School of Civil and Env. Eng., Yonsei University, Seoul, Korea

<sup>5</sup> Daehong Kim, Senior Researcher, Korea Electric Power Corporation, Daejeon Korea

Lee (1991) investigated the group efficiency of reticulated micropiles, which changed with pile spacing and pile length. It was observed that the group efficiency changed with pile spacing (S). The highest group efficiency was observed for the pile spacing equal to 8D.

Forever (2002) which national project conducted in France presented several experimental researches in full-scale and reduced-scale conditions. From the test results, the group efficiency of micropiles less than or close to 1, but only the groups with a large number of micropiles had efficiency greater than unity.

The group efficiency increased with increasing pile length up to around 8 times the width of pile cap. Tsukada et al. (2006) also investigated the performance of micropiles for the bearing capacity of spread footings reinforced with micropiles. According to them, the group efficiency of micropiles changed with pile rigidity, pile embedded angle and soil conditions. It was found that the optimized and effective pile embedded angles were and changed in the range between 15 and 30 degree, depending on settlement levels. The pile embedded angle equal to 30 degree was effective for settlements equal to 10% of foundation width, whereas 15 degree was more effective for settlements equal to 20% of foundation width. The previous results reported in the literatures indicate that the group effects of micropiles can be changed with various foundation geometry and soil conditions.

In the present study, the effects of pile embedded angle and pile spacing on load responses of micropiles were investigated using axial load tests conducted on model micropiles considering various embedded conditions. The focus was given on the load capacity and settlement of micropiles. Results from the tests are presented with discussion on the effects of combined pile geometry conditions.

## **TESTING PROGRAM**

### **Test types and conditions**

An experimental testing program was established to analyze the load capacity and settlement of micropiles for various foundation conditions. To investigate and account for the effect of pile cap or raft, the tests were conducted using different types of foundations including unpiled mat, group micropiles and micropiled raft. These are described in Figure 1. The soil specimens used in the axial load tests were prepared within a chamber with the width and height equal to 1 and 0.7 m, respectively. Uniformly formed dense soil specimens were used, which were prepared by raining sand particles into the square chamber at a predetermined fall heights.

The widths and height of square-shaped mat were 100 and 30 mm, and the diameter and length of micropiles were 5 and 330 mm, respectively. For the micropiles, sand particles were glued to the surfaces of micropiles to simulate the actual rough surface condition of

grouted borehole surface. The detailed configurations of test models are shown in Figure 2. The tests conducted in this study can be summarized into three groups as follows:

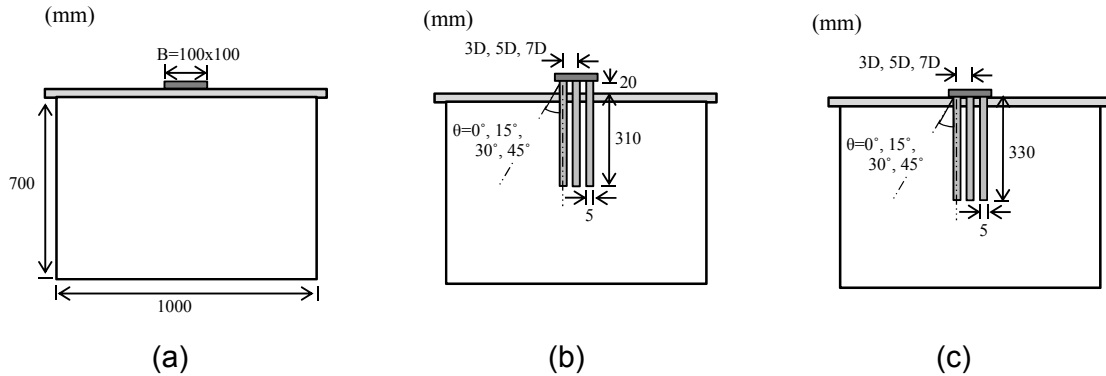


Figure 1 Detailed configuration of axial load tests: (a) unpiled raft; (b) group micropiles; and (c) micropiled-raft.

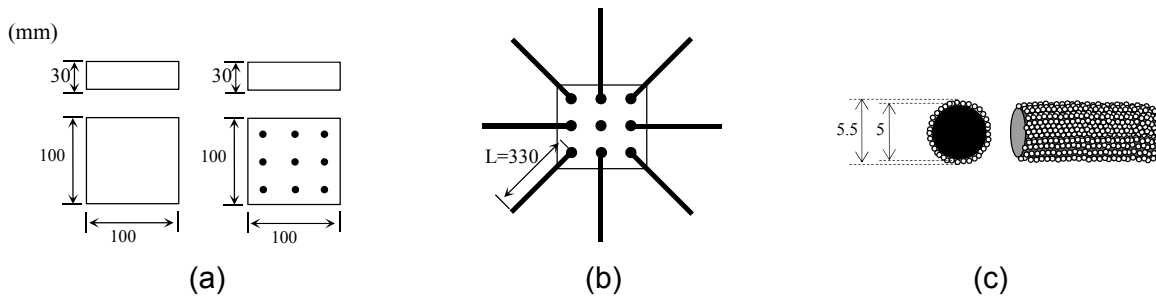


Figure 2 Detailed model configurations : (a) Model raft (pile cap) and micropiled-raft; (b) top view for typical micropiled-raft (N=9, L=330mm); and (c) Model micropile

### a. Axial load tests on unpiled mat

The 100-mm square mat was used in these tests. Once the sand specimen was formed within the test chamber, the mat was placed on the top surface of the specimen and axial load applied on the mat using the loading device.

### b. Axial load tests on group micropiles (GMP)

In these tests, group micropiles were used with various geometry conditions. The soil specimens were prepared in the same way as used for the unpiled mat. Group micropiles were installed at equal pile spacing and embedded angle. In order to consider and measure the load capacity of micropiles only, the pile cap was installed 20 mm above the top surface of soil specimen as indicated in Figure 1(b). The micropiles were installed in the model soil specimen fixing with installation frames. There are described the procedures for setting the group micropile in Figure 3. Three pile spacing distances of 3D, 5D and 7D and four pile embedded angles of 0, 15, 30 and 45 degrees were considered.

### c. Axial load tests on micropiled-raft (MPR)

The micropiled-rafts were the same as the group micropiles except that the raft (pile cap) was placed on the surface allowing the mobilization of load carrying capacity. The pile spacing distances were equal to 3D, 5D and 7D, and the embedded pile angles were 0, 15, 30 and 45 degrees. The axial load was applied until the settlement reached 20 mm.



Figure 3 Procedure for axial load tests : (a) Making the model specimen; (b) Installation of micropiles; (c) Completion of group micropile; and (d) Performance of axial load tests

### **Soil conditions**

The test sand was Jumunjin sand, a clean silica sand. Detailed properties of the test sand are given in Table 1. The values of  $\phi'$  were obtained from the triaxial tests that were conducted at dense and loose conditions with  $D_R = 58\%$  and  $90\%$ . Based on the results from the triaxial tests, the following correlation was obtained for the evaluation of  $\phi'$  as a function of relative density  $D_R$ :

$$\phi' = 0.034 \cdot D_R + 37.03 \quad (1)$$

Table 1 Basic properties of test sand.

Max. void ratio ( $e_{max}$ )	0.927
Min. void ration ( $e_{min}$ )	0.591
Specific gravity ( $G_s$ )	2.65
$D_{10}$ (mm)	0.335
$D_{50}$ (mm)	0.525
Uniformity coefficient ( $C_u$ )	1.73
Curvature coefficient ( $C_c$ )	0.97
Max. dry unit weight ( $kN/m^3$ ) ( $\gamma_{max}$ )	16.34
Min. dry unit weight ( $kN/m^3$ ) ( $\gamma_{min}$ )	13.49
Soil type (USCS)	SP

## TEST RESULTS AND ANALYSIS

### Variation of load capacity

Figure 4 shows the load-displacement curves for unpiled mat, Group micropile (GMP) and Micropiled-raft (MPR). The load capacities of unpiled mat and MPR were determined at the settlement equal to 10% of mat width. The load capacity of GMP was also measured at the same settlement to compare the load capacities applying the consistent criterion.

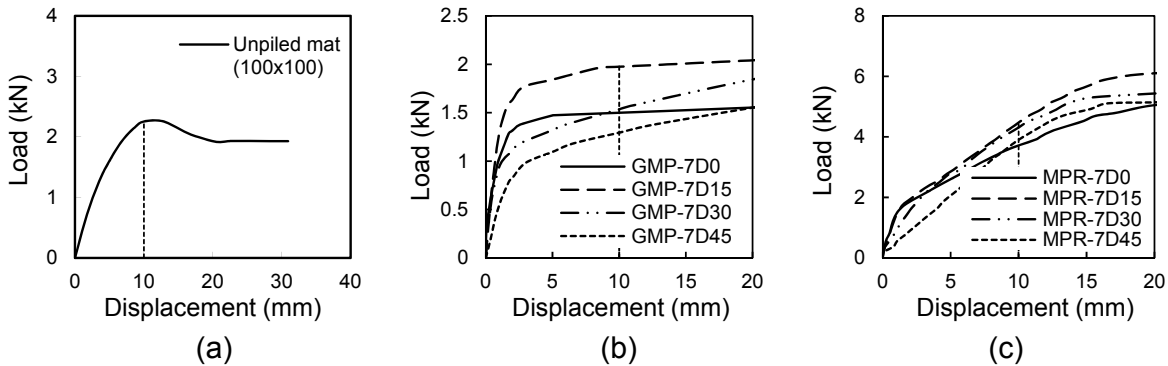


Figure 4 Load-displacement curves : (a) Unpiled mat; (b) Group micropiles; and (c) Micropiled-rafts

Figure 5 shows the results from the axial load tests. The load capacity of MPR and its variation as a function of pile embedded angle are given in Figure 5(a). The load capacity ratios between MPR, mat and GMP are shown in Figure 5(b), which represent changes in load capacity due to the interactions between micropiles and raft. As shown in Figure 5(a), the load capacity of MPR changed with pile spacing and embedded pile angle. It increased with increasing pile spacing and pile embedded angle up to 15 degree. After the 15 degree of pile embedded angle, the load capacity of MPR became decreasing. When the embedded pile angle was equal to 45 degree, the load capacities were even slightly lower than for 0 degree.

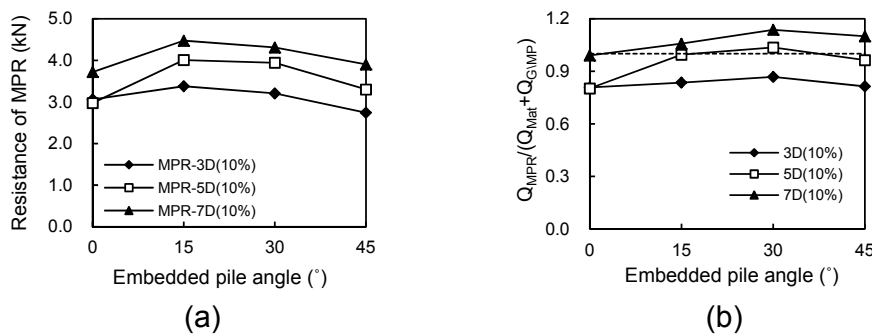


Figure 5 The resistance and group effect for micropiled-raft(MPR) : (a) Resistance of micropiled-raft (MPR); (b) The load capacity ratios between MPR, mat and GMP

From the comparison of the load capacities for GMP, MPR and mat in Figure 5(b), it can be seen that the load capacity of MPR was around 80% of the summed load capacity of unpiled mat and GMP at the pile spacing equal to 3D. However, for the pile spacing and embedded angle greater than 5D and 15 degree, higher load capacities of MPR than others were observed. According to the test results obtained in this study, the load capacity of micropiles, in particular when the pile cap is used, is largely affected by both embedded angle and pile spacing. It was shown that there is an certain optimized range of these foundation geometry parameters that tend to produce higher load capacity.

### **Settlement reduction of micropiled-raft**

Figure 6 shows changes in induced settlement MPR compared with unpiled mat. The settlements of MPR and unpiled mat (i.e.,  $S_{MPR}$  and  $S_{Mat}$ ) in Figure 6 were all measured at the same load level equal to resistance of unpiled mat. As shown in Figure 6, induced settlements of MPR changed with pile spacing and embedded pile angle. The reductions in settlement for MPR in comparison to those of mat increased with increasing pile spacing. For the cases with pile spacing equal to 3D, the reduction ratio ( $S_{MPR}/S_{Mat}$ ) varied in the range of 0.4 to 0.8 while the range of reduction ratio from 0.38 to 0.6 was observed for pile spacing equal to 5D and 7D.

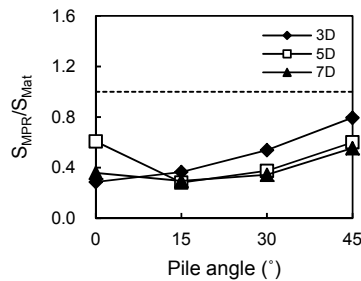


Figure 6 Settlement reduction of micropiled-raft

### **CONCLUSION**

In this paper, the load capacity of micropiles and its variation with various foundation geometry conditions were investigated based on the experimental test results. The pile embedded angle and pile spacing were selected and analyzed as main influence configuration parameters in the testing program. Although the test results had a limitation for scale effects due to use the small scale models, it was observed that the load capacity of MPR increased with increasing pile spacing and embedded pile angle up to the pile embedded angle equal to 15 degrees. After this pile embedded angle, the load capacity decreased for all pile spacing distances considered in the tests.

The load capacity of MPR was around 80% of the summed load capacity of mat and GMP at the pile spacing equal to 3D. The test results in this study indicated that the effective pile

embedded angle is between 15 and 30 degrees in regards to the mobilization of load carrying capacity.

The settlement reduction effect of MPR changed with pile spacing and pile embedded angle. When the pile cap contributed to the load carrying behavior, more settlement reduction was observed as pile spacing became larger.

## **ACKNOWLEDGEMENTS**

This work was supported by a research grant from Korea Electronic Power Corporation (KEPCO) and the National Research Foundation of Korea (NRF) grant funded by the Korea government (MSIP) (No. 2011-0030040).

## **REFERENCE**

FHWA (2005). "Micropile Design and Construction Reference Manual." U.S. Department of Transportation Federal Highway Administration, FHWA NHI-05-039.

Forever (2002), "Synthesis of the results of the national project on micropiles", Research Report, IREX

Lee, W. T. (1991), "A Study on reinforcing effect of reticulated root piles on shallow footing", a doctor's thesis, Seoul National Univ.

Lizzi, F. and Carnevele, G. (1979), "Les Reseaux de Pieux Racines Pour la Consolidation des sols, Aspects Theoretique et Essais sur Mondile", Proc. Int. Conf., Soil Reinforcement, Paris, Vol.2, pp.317-324.

Tsukada, Y., Miura, K., Tsubokawa, Y., Otani, Y. and You, G.L. (2006), "Mechanism of bearing capacity of spread footings reinforced with micropiles", Soils and Foundations, Vol. 46, No. 3, 367-376